Iranian Journal of Catalysis 8(3), 2018, 221-229

IRANIAN JOURNAL OF CATALYSIS

A novel and eco-friendly *o*-phenylendiamine stabilized on silica-coated magnetic nanocatalyst for the synthesis of indenoquinoline derivatives under ultrasonic-assisted solvent-free conditions

Ali Maleki*, Reza Ghalavand, Razieh Firouzi-Haji

Catalysts and Organic Synthesis Research Laboratory, Department of Chemistry, Iran University of Science and Technology, Tehran 16846-13114, Iran.

Received 1 March 2018; received in revised form 14 July 2018; accepted 22 July 2018

ABSTRACT

In this study, a novel and environmentally benign *o*-phenylendiamine stabilized on silica-coated Fe_3O_4 magnetic nanocatalyst (Fe_3O_4@SiO_2@propyltriethoxysilane@*o*-phenylendiamine-SO_3H/HCl) as a hybrid magnetic organometallic nanocatalyst has been synthesized. After that, the structure of this new catalyst was completely characterized via Fourier transforms infrared (FT-IR) spectroscopy, Brunauer–Emmett–Teller (BET), atomic force microscopy (AFM), field-emission scanning electron microscopy (FE-SEM) images, energy dispersive X-ray (EDX) and vibrating sample magnetometer (VSM) analyses. The SEM image of the synthesized nanocatalyst showed that it has a nearly core-shell spherical shape and uniform size distribution with an average size about 40 nm. The BET result revealed that it has 34.88 m^2/g specific surface areas. Finally, its catalytic activity was investigated for the selective synthesis of 7-aryl-8*H*-benzo[h]indeno[1,2-b]quinoline-8-one derivatives in high-to-excellent isolated yields under solvent-free conditions and ultrasound irradiation at room temperature. This nanocatalyst can be easily recovered from the reaction mixture using an external magnet and reused for at least eight times without significant decrease in catalytic activity.

***Keywords**: Magnetite heterogeneous nanocatalyst, Ultrasonic irradiation, Benzo-indeno-quinolineone, Multicomponent reaction, Green synthesis.*

1. Introduction

Nowadays, much attention has been paid to use of ultrasonic irradiation, as a green technique, by scientific and industrial researchers due to its valuable applications in organic synthesis. There are many advantages such as fast, simple and more convenient procedure in this protocol in comparison with traditional methods. There are many reports of organic reactions, which were carried out in higher yields, shorter reaction times or milder conditions under ultrasonic irradiation. Noteworthy, the ultrasonic irradiation results from the acoustic cavitation, which is the formation, growth and collapse of bubbles in liquid. In the other words, the increase of temperature and pressure over a short time in the acoustic cavitation leads to an increase in the rate of chemical reactions and mass transfer [1-4].

*Corresponding author email: maleki@iust.ac.ir
Tel.: +98 21 7724 0540; Fax: +98 21 7302 1584

As a result, due to these unique properties, it is considered an efficient reaction medium for a green, economical and environmentally benign method in organic reactions.

Homogeneous acid catalysts such as Lewis and Brønsted acids, a very important class of catalysts, are commonly used in the chemical industry. However, the separation and recovery of catalysts from the reaction mixture are major drawbacks of these catalysts. Applying heterogeneous catalysts is the best way to overcome this drawback. Recently, heterogeneous acid catalysts have received much attention because of high reactivity, operational simplicity, low toxicity, non-corrosive nature and the potential of the catalyst to be recycled [5,6].

Recently, magnetic nanoparticles (MNPs) have received considerable interest in the field of catalysis science and technology [7,8]. They have the advantages of both homogeneous and heterogeneous catalysts such as high

dispersion, high reactivity and easy separation due to their magnetic properties and nanoscale size [9-12]. Despite nanoparticles have excellent catalytic activities because of higher surface-to-volume ratio, they aggregate due to their higher surface energy; this event reduces their catalytic activities. In order to resolve this defect, various organic and inorganic compounds are usually immobilized onto the active surface of MNPs such as Fe_3O_4. Noteworthy, surface modifying of Fe_3O_4 nanoparticles with inorganic compounds such as silica shells improves the chemical stability of Fe_3O_4 nanoparticles and will increase the available active site of the catalyst for more modification [13].

Multicomponent reactions (MCRs) have attracted much attention due to their valuable characteristics such as simplicity, straightforward reaction model, atom economy, short reaction time, saving cost and energy and production of complex structures [14]. MCRs are the most powerful strategy in green chemistry and in the recent years, these reactions are applied in material, medical and modern synthetic organic chemistry [15,16]. Moreover, these reactions are used for the synthesis of heterocyclic compounds.

Recently, the quinoline nucleus has significant importance in medicinal chemistry and many quinoline containing compounds which provide wide range of pharmacological properties such as anti-malarial, anti-asthmatic, anti-bacterial and anti-hypersensitive activities. Also they have been used in diverse areas of chemistry. Among these compounds, indenoquinolines are one of the most important groups of quinoline derivatives; due to their wide range of medicinal activities such as anti-tumor [17], anti-malarial [18] and inhibitor of steroid reductase, several synthesis methods of indenoquinoline skeletons have been reported. [19,20] and most of these methods require refluxing conditions, organic solvents, expensive catalysts, use of homogeneous catalyst, several steps and tedious work-up procedure [21]. It should be noted that, using tribromomelamine (TBM) as a homogeneous catalyst leads to many problems, including environmental pollution and difficult separation. Furthermore, the design of environmentally benign, simple and high-yielding methods in the presence of heterogeneous catalyst is important for both economical and environmental points of view [22-30].

In continuation of our research on the introduction of new recoverable organometallic nanocatalysts and their applications in organic synthesis [31-34], herein, we report a convenient and efficient method for the synthesis of *o*-phenylendiamine stabilized on silica-coated Fe_3O_4 MNP catalyst (Fe_3O_4@SiO_2@propyltriethoxysilane@*o*-phenylendiamine (OPSF)-SO_3H/HCl) as a super paramagnetic heterogeneous nanocatalyst. Then, it was characterized and applied in a multicomponent one-pot synthesis of 7-aryl-8*H*-benzo[h]indeno[1,2-b]quinoline-8-ones derivatives **4a–l** starting from 1,3-indanedione, aromatic aldehydes and 1-naphthylamine under solvent-free conditions and ultrasound irradiation in high-to-excellent yields at room temperature (Scheme 1). This synthesized nanocatalyst was easily separated from the reaction mixture by using a small external magnet and applied at least eight times without significant loss of catalytic activity. To the best of our knowledge, this is the first report of design, preparation, and characterization OPSF-SO_3H/HCl nanocatalyst and its application as a heterogeneous catalyst in the synthesis of 7-aryl-8H-benzo[h]indeno[1,2-b]quinoline-8-ones derivatives.

2. Experimental

2.1. General

All the solvents, chemicals and reagents were purchased from Merck, Sigma and Aldrich. Melting points were measured on an Electrothermal 9100 apparatus and are uncorrected. Fourier transforms infrared spectroscopy (FT-IR) spectra were recorded on a Shimadzu IR-470 spectrometer by the method of KBr pellet. ^{1}H nuclear magnetic resonance (NMR) spectra were recorded on a Bruker DRX-500 Avance spectrometer at 500 MHz. Field-emission scanning electron microscopy (FE-SEM) images were taken with the Sigma-Zeiss microscope with the attached camera.

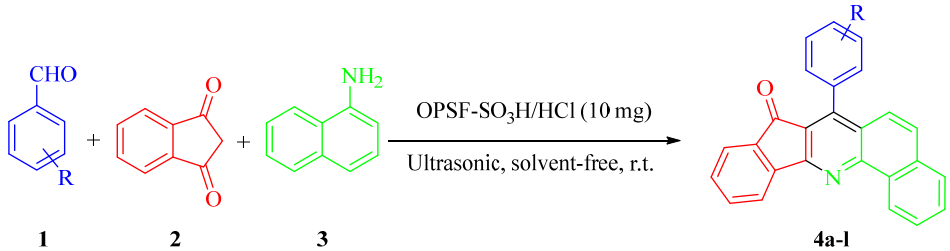

Scheme 1. Synthesis of 7-aryl-8*H*-benzo[h]indeno[1,2-b]quinoline-8-ones derivatives **4a–l** in the presence of OPSF-SO_3H/HCl nanocatalyst.

Magnetic measurements of the solid samples were performed using Lakeshore 7407 and Meghnatis Kavir Kashan Co., Iran vibrating sample magnetometers (VSMs). The elemental analysis of the nanocatalyst was carried out by energy-dispersive X-ray (EDX) analysis recorded on Numerix DXP-X10P. Moreover, the tip radii were obtained from the direct AFM measurements of the tip apex region in tapping mode. The shell surface was mounted on the AFM stage and the Triboscope recording unit with transducers and leveling device was placed on the top of a NanoScope III E 164 | 164 mm 2 XY piezo scan base. The BET surface area of the synthesized nanomaterial was characterized by an ASAP 2020 specific surface area and porosity analyzer (Micromeritics Instrument Corp.), and the samples were degassed for 6h at 469.86 K.

2.2. Preparation of Fe_3O_4 nanoparticles

The Fe_3O_4 nanoparticles were synthesized via the co-precipitation of $FeCl_3$ and $FeCl_2{\cdot}4H_2O$ at a molar ratio of 2:1 in the presence of ammonia. Typically, 2.82 g of $FeCl_3$ and 1.72 g of $FeCl_2{\cdot}4H_2O$ were mixed in 80 mL of distilled water and vigorously stirred at 80 ℃ with a mechanical stirrer. After the temperature had reached 80 ℃, 10 mL ammonia was added drop wise to the mixture. The mixture was then stirred for another 40 min and then cooled to room temperature. The black precipitate was collected using an external magnet and washed several times with ethanol and distilled water. The black product was dried at 80 ℃ in an oven.

2.3. Preparation of Fe_3O_4@SiO_2 nanoparticles

First, 45 mg of Fe_3O_4 nanoparticles were dispersed in 16 mL of deionized water by using an ultrasonic water bath, after that 2 mL of aqueous ammonia solution (25 wt%) and 80 mL of ethanol were added to the reaction mixture. Next, 0.8 mL of TEOS was added drop wise into the Fe_3O_4 nanoparticle solution under vigorous stirring at room temperature. The mixture was then stirred for 24 h at room temperature. The products were separated by an external magnet and washed several times with distilled water. The final product was collected and dried at 50 °C.

2.4. Preparation of Fe_3O_4@SiO_2@3-chloropropyl triethoxysilane nanoparticles

Initially, 0.292 g of as-obtained Fe_3O_4@SiO_2 nanocomposite was added in 10 mL THF. Then, 0.24 g of NaH was dispersed in to the mixture by ultrasonication. After that, 2 mL of 3-chloropropyltriethoxysilane was added drop-wise at room temperature and stirred for another 16 h at 60 °C. The resultant products were separated by an external magnet and washed with ethanol and deionized water in sequence, and then the precipitation was dried under vacuum at 60 °C for 2 h for further action.

2.5. Preparation of OPSF nanocatalyst

First, 0.25 g of Fe_3O_4@SiO_2@$OSi(CH_2)_3Cl$ was dispersed in 25 mL EtOH in three separate flasks. Then, 0.25 mmol (27 mg) of *o*-phenylenediamine (OPDA) was added to each of dispersions and refluxed for 12 h. The obtained mixture was filtered and washed with the excessive amount of EtOH and dried at 60 °C for 12 h [30].

2.6. Preparation of OPSF-SO_3H/HCl nanocatalyst

Finally, the chlorosulfonic acid (10 mmol) was added dropwise to the synthesized OPSF nanocatalyst in dry dichloromethane and the mixture was stirred for 6 h. After completion of several steps of filtering, washing and drying, the intended OPSF-SO_3H/HCl nanocatalyst was obtained [35]. The synthesis method is illustrated in Scheme 2.

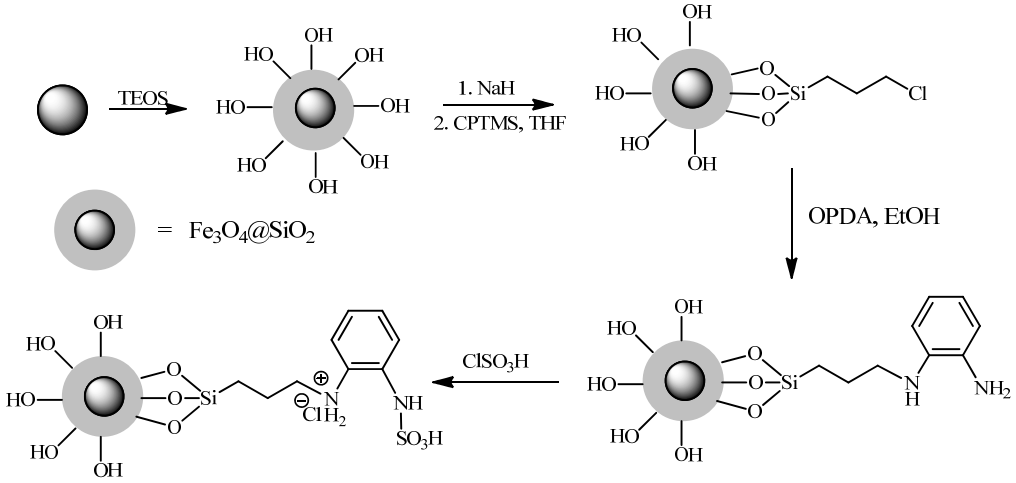

Scheme 2. Synthesis of OPSF-SO_3H/HCl nanocatalyst.

*2.7. General procedure for the synthesis of 7-aryl-8H-benzo[h]indeno[1,2-b]quinoline-8-one derivatives **4a–l***

A mixture of an aromatic aldehyde **1** (1 mmol), 1,3-indanedione **2** (1 mmol, 0.15 g), 1-naphthylamine **3** (1 mmol, 0.14 g) and OPSF-SO_3H/HCl nanocatalyst (0.010 g) react in an ultrasonic bath at room temperature under solvent-free conditions. The completion of the reaction was monitored by the thin layer chromatography (TLC). After completion of the reaction, the catalyst was easily separated by an external magnet. The pure products were obtained from the reaction mixture by recrystallization from hot EtOH and no more purification was required. All the products were compounds which were identified by characterization of their melting points (as indicated in Table 3), comparison with those authentic literature samples and also in some cases their FT-IR.

3. Results and Discussion

In this work, an environmentally benign *o*-phenylendiamine was stabilized on silica-coated Fe_3O_4 MNP catalyst (Fe_3O_4@SiO_2@propyltri ethoxysilane@*o*-phenylendiamine-SO_3H/HCl) as a hybrid magnetic organometallic nanocomposite. Initially, the immobilization of a base group (*o*-phenylendiamine) onto magnetic nanoparticle (Fe_3O_4) in several steps occurred. After that, the chlorosulfonic acid was added dropwise to Fe_3O_4@SiO_2@propyltriethoxysilane@ *o*-phenylendiamine (OPSF) in dry dichloromethane and the mixture was stirred for 6 h to prepare the magnetic nanocatalyst. This finalized nanocatalyst was an effective catalyst in the synthesis of 7-aryl-8H-benzo[h]indeno[1,2-b]quinoline-8-ones derivatives.

3.1. Characterization of the prepared OPSF-SO_3H/HCl nanocatalyst

The OPSF-SO_3H/HCl nanocatalyst was prepared after several steps. The FT-IR spectroscopy was utilized to analyze and confirm functional groups of the finalized OPSF-SO_3H/HCl nanocatalyst. As can be seen in Fig. 1, a peak exhibited at 584 cm^{-1} belongs to the Fe–O–Fe stretching vibration. In addition, two strong peaks appeared at 1085 and 1151 cm^{-1} are attributed to Si–O–Si asymmetric stretching vibration. The bands appeared at 2923 and 2854 cm^{-1} are related to the stretching vibration of C-H bonds. Moreover, the asymmetric stretching vibrations of O–H and N–H groups are also observed at 3380 cm^{-1} [30]. Furthermore, the S-O stretching vibrations of SO_3H groups in OPSF-SO_3H/HCl nanocatalysts on the OPSF surface appeared at 1010–1120 cm^{-1}.

Furthermore, acidity ($[H^+]$) of the synthesized OPSF-SO_3H/HCl nanocatalysts was evaluated by the back titration method. Initially, 0.5 g of nanocatalyst, 0.5 g of NaCl and 10 mL of NaOH (0.1 M) were added to 20 mL of distilled water and stirred for 24 h on a magnetic stirrer. After that, three drops of phenolphthalein were added to it and color of the mixture was changed to pink. Then, it was titrated by a solution of HCl (0.1 M) until it reached to neutral pH. After calculations, pH value of the related nanocatalyst was found to be 1.82.

The morphology and size details of the nanocatalyst were investigated by FE-SEM measurement, which is illustrated in Fig. 2. FE-SEM image is shown that the OPSF-SO_3H/HCl nanocatalyst has a nearly spherical shape and uniform size distribution with an average size of 36.4 ± 10 nm.

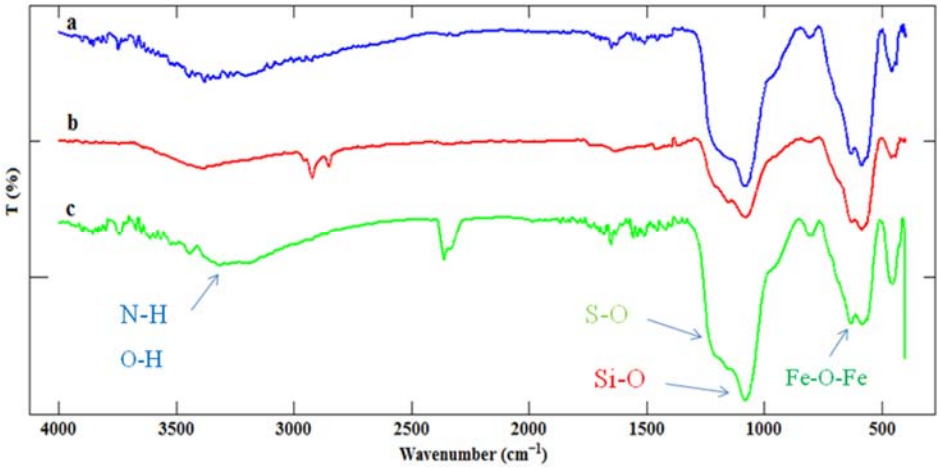

Fig. 1. FT-IR spectra of: (a) Fe_3O_4, (b) OPSF and (c) OPSF-SO_3H/HCl.

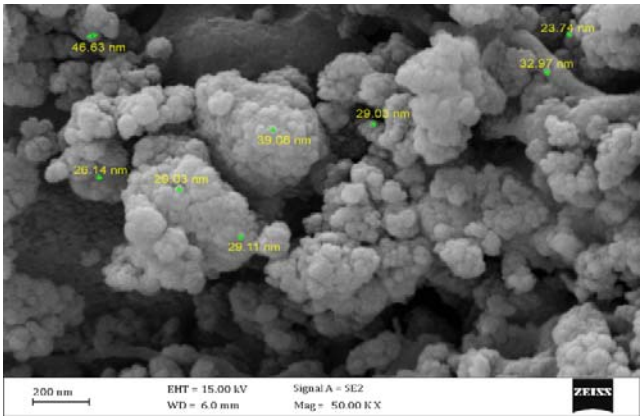

Fig. 2. FE-SEM image of OPSF-SO_3H/HCl nanocatalyst.

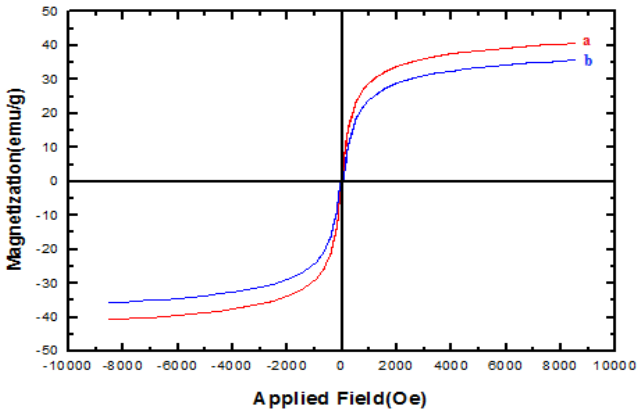

Fig. 4. VSM magnetization curve of (a) OPSF and (b) OPSF-SO_3H/HCl magnetic nanoparticles.

The result of the EDX analysis of the OPSF-SO_3H/HCl magnetic nanoparticles is illustrated in Fig. 3. It confirms the presence of iron, carbon, oxygen, nitrogen, sulfur, chlorine and silicon elements in the nanocatalyst.

The magnetic properties of OPSF-SO_3H/HCl nanocatalyst were measured by VSM curves at room temperature. As can be seen in Fig. 4, the hysteresis loops of the superparamagnetic behavior can be clearly observed for the prepared magnetic nanoparticles. The superparamagnetism is responsible for an applied magnetic field without retaining any magnetism after removal of the applied magnetic field. Based on M versus H curves, the saturation magnetization value (Ms) of uncoated MNPs was found to be 56 emu g^{-1} [26]. The saturation magnetization of OPSF and OPSF- SO_3H/HCl nanoparticle were 40.73 and 35.733 emu g^{-1}, respectively. These were lower than neat Fe_3O_4 nanoparticles. As a result, this decrease in the saturation magnetization value is mainly attributed to the presence of materials on the surface of the nanoparticles.

As can be seen in Fig. 5, the nanostructure surface of OPSF-SO_3H/HCl magnetic nanoparticles was confirmed by AFM analysis. It was found that, after sulfonation of OPSF nanoparticles, these magnetic nanoparticles maintain their morphological properties. A 10 µm×10 µm image of nanoparticles was displayed as a three dimensional projection.

Specific surface areas of the OPSF-SO_3H/HCl magnetic nanoparticles were evaluated with the BET analysis method. It was found that the surface area value of this synthesized magnetic nanoparticles is 34.88 m^2/g with pore volume of 0.12 cm^3/g and pore size 12.52 nm.

3.2. Catalytic application of OPSF-SO_3H/HCl nanocatalyst in the synthesis of 7-aryl-8H-benzo[h]indeno[1,2-b]quinoline-8-one derivatives

The three-component reaction of 1,3-indanedione, 4-chlorobenzaldehyde and 1-naphthylamine was chosen as the model reaction for optimization of the reaction conditions (**4a**). As can be seen in Table 1, we investigated the effects of the various solvents on the reaction.

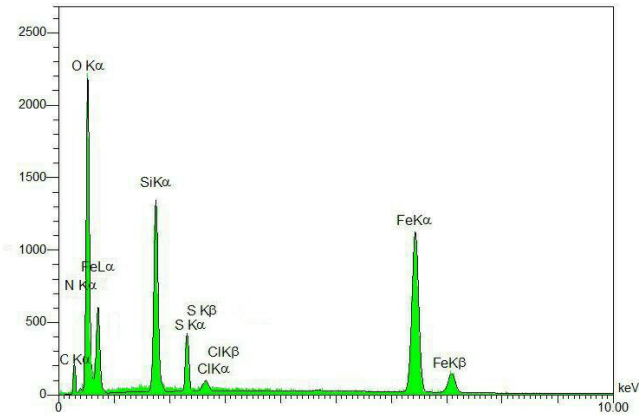

Fig. 3. EDX analysis of OPSF-SO_3H/HCl magnetic nanoparticles.

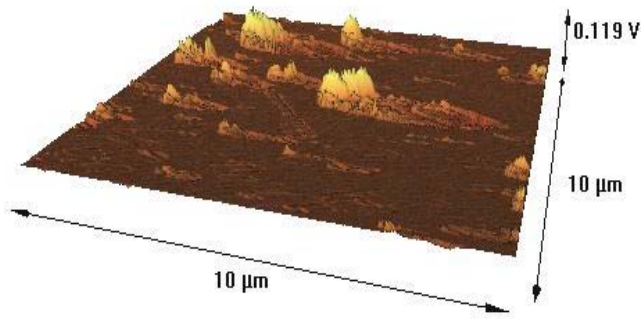

Fig. 5. AFM image of OPSF-SO_3H/HCl magnetic nanoparticles.

Table 1. Optimizing of the reaction conditions in the synthesis of 7-aryl-8H-benzo[h]indeno[1,2-b]quinoline-8-ones derivatives under ultrasound irradiation.

Entry	Solvent	Temp. (°C)	Yield (%)[a]
1	Water	r.t.	40
2	Ethanol	r.t.	95
3	Solvent-free	r.t.	98
4	Solvent-free	50	98
5	Solvent-free	80	99

[a]Isolated yield.

According to the results illustrated in Table 1, the optimized conditions for the reaction will be obtained in ultrasonic bath at room temperature under solvent-free conditions.

Moreover, the effect of the catalyst amount was evaluated on the reaction yield. It was found in Table 2 (entry 1-4), that using 10 mg of the OPSF-SO_3H/HCl nanocatalyst is applicable to complete the reaction after 5 min in 98% yield under solvent-free conditions and ultrasound irradiation at room temperature. Finally, to compare the efficiency of this synthesized catalyst with that of some previously reported catalysts for the synthesis of 7-aryl-8*H*-benzo[h]indeno [1,2-b]quinoline-8-one derivatives, as can be seen in Table 2 (entry 5-9), we bring the results for these catalysts in the synthesis of **4a** as a model reaction. The results clearly demonstrate the superiority of the present work under ultrasound irradiation in saving time, energy and high yields of the products.

After optimizing the reaction conditions, we investigated the generality of these conditions using various aromatic aldehydes. The results are summarized in Table 3. It was found that aromatic aldehydes carrying both different electron-donating and electron-withdrawing groups were subjected to the condensation and in all cases the desired products were obtained in high-to-excellent yields after appropriate reaction times.

Table 2. Comparison of some catalysts effects with OPSF-SO_3H/HCl nanoparticles of the model reaction.

Entry	Conditions	Catalyst amount	Time (min)	Yield (%)[a]	Ref.
1	Solvent-free, stirring, r.t.	-	10	Trace	This work
2	Solvent-free, ultrasound, r.t.	-	10	35	This work
3	$FeCl_3$, solvent-free, ultrasound, r.t.	10 mg	10	40	This work
4	$FeCl_2$, solvent-free, ultrasound, r.t.	10 mg	10	30	This work
5	Fe_3O_4, solvent-free, ultrasound, 40°C	30 mg	90	68	[29]
6	Fe_3O_4@SiO_2, solvent-free, ultrasound, r.t.	10 mg	90	50	This work
7	OPSF-SO_3H, solvent-free, ultrasound, r.t.	5 mg	5	85	This work
8	OPSF-SO_3H, solvent-free, ultrasound, r.t.	10 mg	5	98	This work
9	OPSF-SO_3H, solvent-free, ultrasound, r.t.	20 mg	5	95	This work
10	OPSF-SO_3H, solvent-free, ultrasound, r.t.	30 mg	5	93	This work
11	OPSF-SO_3H, solvent-free, stirring, 40°C	10 mg	10	90	This work
12	OPSF, solvent-free, ultrasound, r.t.	10 mg	5	90	This work
13	Fe_3O_4@cellulose-OSO_3H, solvent-free, stirring, 40°C	30 mg	5	40	[29]
14	TBM, solvent-free, stirring, 80 °C	15 mg	45	94	[21]
15	P(4-VPH)HSO_4, EtOH, stirring, reflux	20 mg	120	86	[36]
16	[$Fe(HSO_4)_3$], DMSO, 90 °C	0.1 mmol	210	90	[37]
17	$H_6P_2W_{18}O_{62}$ $18H_2O$, Acetic acid, reflux	0.01 mmol	360	96	[38]

[a]Isolated yield.

Table 3. Synthesis of 7-aryl-8*H*-benzo[h]indeno[1,2-b]quinoline-8-one derivatives using OPSF-SO_3H/HCl nanoparticles as catalyst.

Entry	R	Product	Yield[a] (%)	m.p. (°C)		Ref.
				Observed	Literature	
1	4-Cl	**4a**	98	244-246	259-261	[39]
2	4-Br	**4b**	95	221-223	218-220	[21]
3	4-Me	**4c**	91	245-247	256-260	[39]
4	4-OMe	**4d**	90	230-233	233-235	[21]
5	4-CN	**4e**	97	242-243	240-241	[29]
6	4-F	**4f**	97	241-242	231-235	[39]
7	3-NO_2	**4g**	95	228-230	222-224	[21]
8	3-Br	**4h**	95	241-243	236-238	[21]
9	3-Cl	**4i**	94	228-230	230-232	[21]
10	3-OH	**4j**	86	231-233	228-229	[39]
11	2-Cl	**4k**	95	284-287	289-291	[39]
12	H	**4l**	92	200-204	202-204	[21]

[a]Isolated yield

The plausible mechanism of the reaction in the presence is shown in Scheme 3. Initially, intermediate **II** is obtained as a result of a Knoevenagel condensation between a carbonyl group of activated aldehyde **1** and 1,3-indanedione **2** in the presence of OPSF-SO_3H/HCl nanocatalyst. After that, the subsequent addition of 1-naphthylamine **3**, followed by cyclization, dehydration and oxidation would afford the indenoquinolines [40-42].

3.3. Reusability of OPSF-SO_3H/HCl nanocatalyst

The reusability of the catalyst is one of the most important advantages for commercial applications. Therefore, the reusability of OPSF-SO_3H/HCl nanocatalyst was evaluated in the model reaction. After completion of the reaction, the nanocatalyst was recovered by an external magnet and washed with ethanol, dried and reused in subsequent reactions at least 8 times without any significant lose in yield of the products (The yields were 98, 97, 95, 93, 90, 88, 86 and 85%, respectively).

4. Conclusions

In summary, a novel and environmentally benign *o*-phenylendiamine stabilized on silica-coated Fe_3O_4 MNP catalyst (Fe_3O_4@SiO_2@propyltriethoxysilane@ *o*-phenylendiamine-SO_3H/HCl) have been synthesized and completely characterized by FT-IR spectroscopy, FE-SEM images, BET, AFM, VSM and EDX analyses. Noteworthy, this nanocomposite has the uniform size with an average size about 40 nm and 34.88 m^2/g specific surface areas. AFM result revealed that these magnetic nanoparticles maintain their morphological properties. Then, the catalytic activity of the nanocomposite was investigated in the synthesis of 7-aryl-8*H*-benzo[h]indeno[1,2-b]quinoline-8-ones. The products were obtained in high-to-excellent yields at room temperature under mild reaction conditions. The nanocatalyst was easily separated by an external magnetic field and reused efficiently for the several times without a significant decrease in catalytic activities. This is the first report on design, preparation, functionalization and characterization of the present nanocomposite and also performance as a heterogeneous catalyst in organic reactions.

Acknowledgements

The authors gratefully acknowledge the partial support of the Research Council of the Iran University of Science and Technology.

References

[1] N. Ghaffari Khaligh, F. Shirini, Ultrason. Sonochem. 22 (2015) 397-403.
[2] J.H. Bang, K.S. Suslick, Adv. Mater. 22 (2010) 1039-1059.
[3] D. Elhamifar, Z. Ramazani, M. Norouzi, R. Mirbagheri, J. Colloid Interf. Sci. 511 (2018) 392–401.
[4] A. Maleki, M. Aghaie, Ultrason. Sonochem. 39 (2017) 534-539.
[5] J. Grunes, J. Zhu, G.A. Somorjai, Chem. Commun. 18 (2003) 2257–2260.
[6] J.A. Melero, R. Grieken, G. Morales, Chem. Rev. 106 (2006) 3790-3812.

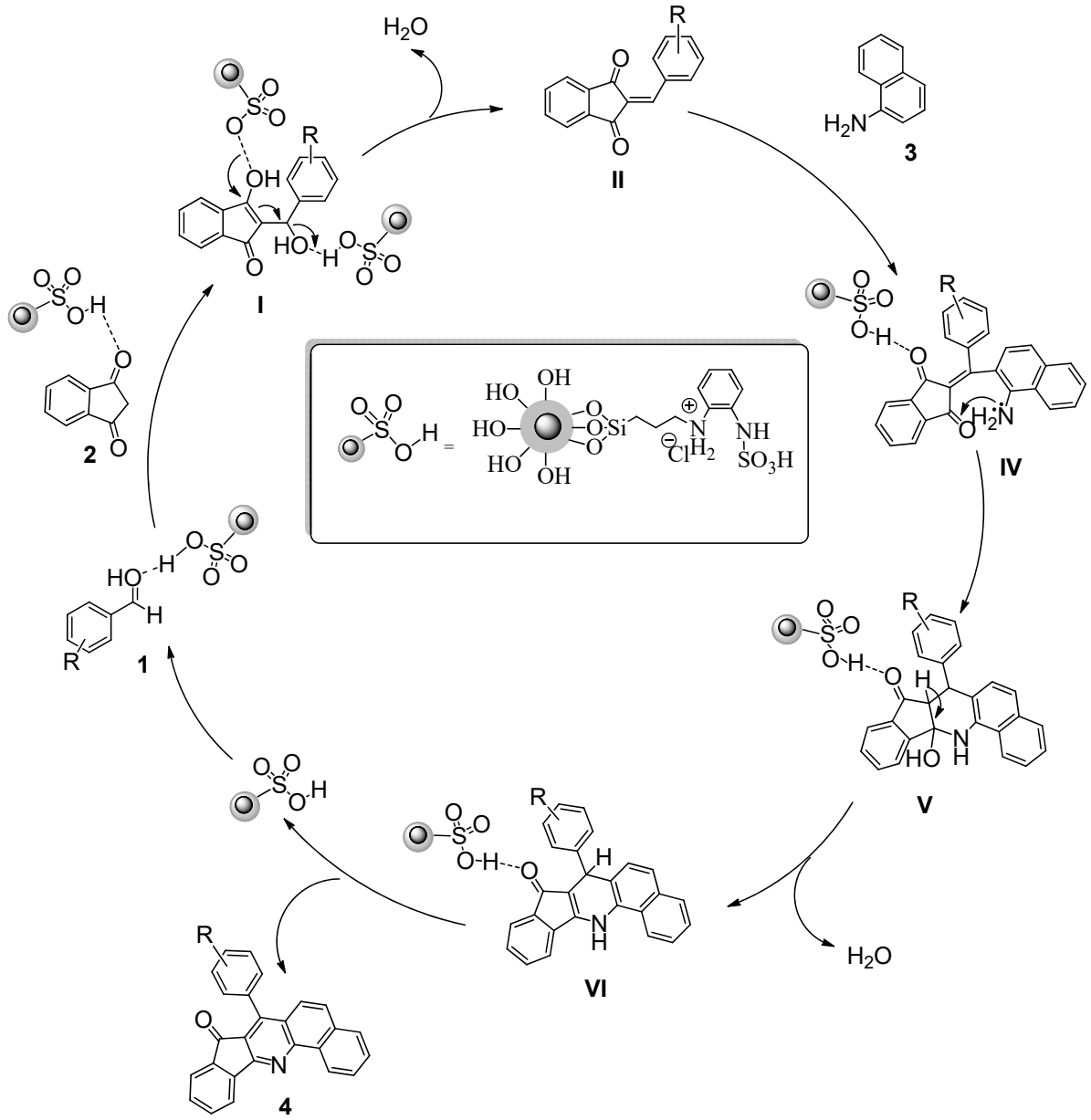

Scheme 3. Proposed mechanism for the synthesis of **4a-l** by using OPSF-SO_3H/HCl.

[7] Y. Zheng, P. D. Stevens, Y. Gao, J. Org. Chem. 71 (2006) 537-542.

[8] R. Abu-Reziq, H. Alper, D. Wang, M.L. Post, J. Am. Chem. Soc. 128 (2006) 5279-5282.

[9] H. Salavati, A. Teimouri, Sh. Kazemi, Iran. J. Catal. 7 (2017) 303-315.

[10] M.A. Ghasemzadeh, M. Azimi-Nasrabad, J. Safaei-Ghomi, Iran. J. Catal. 6 (2016) 203-211.

[11] A. Zare, F. Abi, V. Khakyzadeh, A.R. Moosavi-zare, A. Hasaninejad, M. Zarei, Iran. J. Catal. 5 (2015) 311-320.

[12] A. Maleki, Z. Alrezvani, S. Maleki, Catal. Commun. 69 (2015) 29-33.

[13] Q. Zhang, J. Kang, B. Yang, L. Zhao, Z. Hou, B. Tang, Chin. J. Catal. 37 (2016) 389-397.

[14] A. Dömling, Chem. Rev. 106 (2006) 17-89.

[15] B.B. Toure, D.G. Hall, Chem. Rev. 109 (2009) 4439-4486.

[16] H. Karimi, Iran. J. Catal. 7 (2017) 121-129.

[17] L.W. Deady, J. Desneves, A.J. Kaye, G.J. Finlay, B.C. Baguley, W.A. Denny, Bioorg. Med. Chem. 8 (2000) 977-984.

[18] R.A. Jones, S.S. Panda, C.D. Hall, Eur. J. Med. Chem. 97 (2015) 335-355.

[19] F. Shi, S. Zhang, S. Wu, Y. Gao, S. Tu, Mol. Divers. 15 (2011) 497-505.

[20] H. Eshghi, M.A. Nasseri, R. Sandaroos, H.R. Molaei, S. Damavandi, Met. Org. Chem. 42 (2012) 573-578.

[21] S.S. Mansoor, M. Ghashang, K. Aswin, Res. Chem. Intermed. 41 (2015) 6907-6926.

[22] A. Maleki, M. Aghaei, Ultrason. Sonochem. 38 (2017) 585-589.
[23] A. Maleki, M. Aghaei, Ultrason. Sonochem. 38 (2017) 115-119.
[24] A. Maleki, Ultrason. Sonochem. 40 (2018) 460-464.
[25] A. Maleki, RSC Adv. 4 (2014) 64169–64173.
[26] A. Maleki, P. Zand, Z. Mohseni, RSC Adv. 6 (2016) 110928-110934.
[27] A. Maleki, E. Akhlaghi, R. Paydar, Appl. Organometal. Chem. 30 (2016) 382–386.
[28] A. Maleki, R. Firouzi Haji, M. Ghassemi, H. Ghafuri, J. Chem. Sci. 129 (2017) 457–462.
[29] A. Maleki, N. Nooraie Yeganeh, Appl. Organometal. Chem. 31 (2017), e3814; DOI: 10.1002/aoc.3814.
[30] A. Maleki, M. Kamalzare, Catal. Commun. 53 (2014) 67-71.
[31] A. Maleki, N. Ghamari, M. Kamalzare, RSC Adv. 4 (2014) 9416-9423
[32] A. Maleki, R. Firouzi-Haji, Z. Hajizadeh, Int. J. Biol. Macromol. 116 (2018) 320-326.
[33] A. Maleki, M. Ghassemi, R. Firouzi-Haji, Pure Appl. Chem. 90 (2018) 387-394.
[34] A. Maleki, Z. Hajizadeh, R. Firouzi Haji, Microporous Mesoporous Mater. 259 (2018) 46-53.
[35] M.A. Zolfigol, R. Ayazi-Nasrabadi, S. Baghery, Appl. Organometal. Chem. 30 (2016) 273-281.
[36] N. Ghaffari Khaligh, Chin. J. Catal. 35 (2014) 474-480.
[37] H. Eshghi, M.A. Nasseri, R. Sandaroos, H.R. Molaei, S. Damavandi, Synth. React. Inorg. Met. Org. Chem. 42 (2012) 573-578.
[38] M.M. Heravi, T. Hosseini, F. Derikvand, S.Y.S. Beheshtiha, F.F. Bamoharram, Synth. Commun. 40 (2010) 2402-2406.
[39] M. Mamaghani, T. Hosseyni Larghani. J. Chem. Res. 36 (2012) 235-237.
[40] M.A. Zolfigol, M. Safaiee, F. Afsharnadery, N. Bahrami-Nejad, S. Baghery, S. Salehzadeh, F. Maleki, RSC Adv. 5 (2015) 100546-100559.
[41] A. Maleki, H. Movahed, P. Ravaghi, P. Carbohydr. Polym. 156 (2017) 259-267.
[42] M. Kiafar, M.A. Zolfigol, M. Yari, A. Taherpour, RSC Adv. 6 (2016) 102280-102291.
[43] M. A. Zolfigol, M. Yari, Appl. Organomet. Chem. 31 (2017) 1-10.